

# Validity of a New Respiratory Resistance Measurement Device to Detect Glottal Area Change

\*Sally J. K. Gallena, †Wei Tian, ‡Arthur T. Johnson, †,§Jafar Vossoughi, ||Stephen A. Sarles, and ¶Nancy Pearl Solomon, \*Baltimore, ‡College Park, §Olney, ||Bethesda, Maryland; Knoxville, Tennessee, and †Seattle, Washington

**Summary: Objective.** To determine the correlation between respiratory resistance ( $R_r$ ) values measured with the Airflow Perturbation Device (APD) to laryngoscopic images of glottal area (GA) in feigned paradoxical vocal fold motion (PVFM), also known as vocal cord dysfunction.

**Hypothesis.** There is a strong inverse relationship between  $R_r$  and GA such that laryngeal constriction can be detected and quantified by APD-measured  $R_r$ .

**Study Design.** Prospective, single subject study.

**Methods.** A healthy adult feigned breathing that was characteristic of PVFM.  $R_r$  and GA were simultaneously recorded, synchronized, and analyzed for three complete breathing cycles with significant glottal constriction occurring during inspiration.

**Results.** Cross-correlation analysis revealed a strong negative correlation ( $-0.824$ ) between GA and  $R_r$  during feigned PVFM breathing such that  $R_r$  increased when GA decreased.

**Conclusion.** APD-measured  $R_r$  appears to be a viable noninvasive method for diagnostic screening and monitoring of treatment outcomes for individuals presenting with dyspnea related to PVFM.

**Key Words:** Paradoxical vocal fold motion–Dyspnea–Respiratory resistance–Airflow Perturbation Device–Glottal area.

## INTRODUCTION

Paradoxical vocal fold motion (PVFM) disorder, previously referred to as vocal cord dysfunction, is a condition where the vocal folds adduct during inspiration and/or supraglottic tissue collapses into the laryngeal airway.<sup>1–5</sup> This action decreases patency at the laryngeal airway causing dyspnea. Based on the clinical symptoms, patients are commonly misdiagnosed as having asthma,<sup>6–8</sup> often leading to long-term use of corticosteroid and bronchodilator medications and inappropriate use of medical resources. When patients fail to respond to asthma therapy, they undergo further diagnostic testing to eventually obtain an accurate diagnosis.

Observation of the larynx through flexible transnasal laryngoscopy or rigid transoral stroboscopy while the patient is symptomatic of PVFM provides the defining criterion for diagnosis.<sup>3,4,8</sup> Provocation challenges such as exercise have been conducted with the flexible scope passed transnasally throughout the challenge,<sup>1,9–11</sup> allowing real-time visual observation of vocal fold motion and laryngeal changes. Although it is the diagnostic gold standard for PVFM, laryngoscopy is invasive and cannot be tolerated by everyone.<sup>12,13</sup> Because of the episodic nature of PVFM, timing the placement of the scope

with the occurrence of symptoms can prevent documentation by laryngoscopic examination despite clinically convincing signs and symptoms.<sup>3</sup> Furthermore, equipment availability and expense may make laryngoscopy prohibitive at some centers or clinics.

Resistance to airflow may be a useful measurement in the assessment of laryngeal airway patency. Respiratory resistance ( $R_r$ ) is the quotient of air pressure (in  $\text{cmH}_2\text{O}$ ) divided by airflow (in L/s) in the pulmonary airways (including upper and lower airways and lung tissue) and is also influenced by resistance provided by the chest wall.<sup>14,15</sup> During resting tidal breathing (RTB) for most individuals without respiratory problems, inspiratory resistance ( $R_i$ ) is slightly lower than expiratory resistance ( $R_e$ ) yielding an inspiratory-to-expiratory ratio less than 1.0.<sup>16</sup> This is consistent with the observation that there is greater vocal fold abduction during inspiration than expiration and slight contraction of the lower airways during expiration.<sup>17</sup> During PVFM, greatly increased inspiratory resistance is expected because laryngeal constriction occurs most dramatically during inspiration.

The Airflow Perturbation Device (APD) was developed by Johnson et al<sup>18</sup> and further refined by Lausted and Johnson<sup>19</sup> to provide accurate, near real-time measures of  $R_i$  and  $R_e$ . Measures of airflow and air pressure detected just downstream of the mouth obtained during breathing cycles are used for the calculation of  $R_r$ .<sup>14</sup> A typical trial requires  $\sim 1$  minute of breathing ( $\sim 500$  perturbations) for the APD to display the mean values for  $R_i$  and  $R_e$ .

Before using the APD for research in patients with PVFM, it is essential to examine whether APD-measured  $R_r$  is sensitive to changes in the laryngeal airway when significant constriction occurs. Specifically, the following question is posed: Does  $R_r$  measured by the APD strongly correlate with glottal area (GA) measurements obtained from two-dimensional aerial images of the larynx? It is hypothesized that laryngeal constriction

Accepted for publication January 10, 2013.

This research was supported in part by National Institutes of Health Grant R43HD062066 awarded to J.V.

From the \*Department of Speech-Language Pathology, Loyola University Maryland, Baltimore, Maryland; †University of Washington, Seattle, Washington; ‡Fischell Department of Bioengineering, University of Maryland, College Park, Maryland; §Engineering and Scientific Research Associates, Olney, Maryland; ||Mechanical, Aerospace and Biomedical Engineering, University of Tennessee, Knoxville, Tennessee; and the ¶Audiology and Speech Center, Walter Reed National Military Medical Center, Bethesda, Maryland.

Address correspondence and reprint requests to Sally J. K. Gallena, Department of Speech-Language Pathology, Loyola University Maryland, 8890 McGaw Road, Baltimore, MD 21045. E-mail: sgallena@loyola.edu

Journal of Voice, Vol. 27, No. 3, pp. 299–304

0892-1997/\$36.00

© 2013 The Voice Foundation

<http://dx.doi.org/10.1016/j.jvoice.2013.01.006>

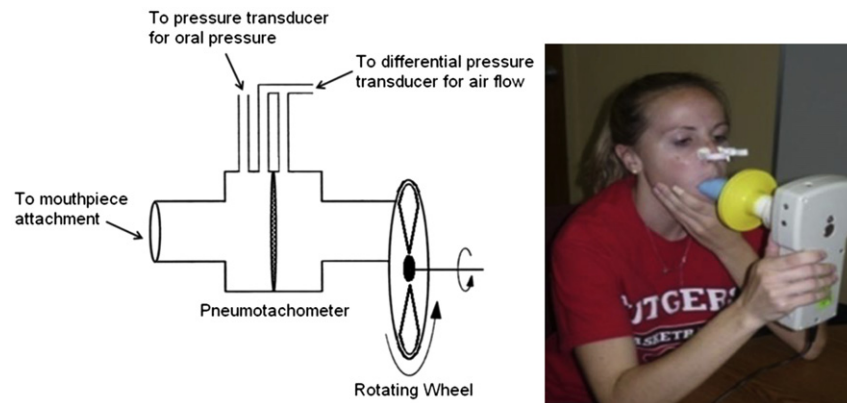


**FIGURE 1.** Schematic of the APD (left) and an athlete using the APD (right) (reprinted with permission by the athlete).

can be detected and quantified by  $R_r$  measured by the APD and that GA and  $R_r$  are inversely related.

## METHOD

### Participant

A healthy 54-year-old woman (the first author) participated in this study that took place at a medical center. A laryngologist confirmed normal laryngeal structure and function in the participant through rigid laryngoscopy. Normal respiratory function was validated by an allergy and asthma physician through pulmonary function tests, which included forced vital capacity, forced inspiratory and expiratory volume in 1 second, and peak inspiratory and expiratory flow. Results from the pulmonary function tests were within normal limits for the participant's age and sex.

### Instrumentation and materials

**Laryngoscope.** A digital chip flexible nasolaryngoscope (70K Series; KayPENTAX, Montvale, NJ) connected to a video stroboscopy system (model 9200C; KayPENTAX) digitally recorded and stored the laryngeal examination to a workstation for playback and analysis.

**Airflow Perturbation Device.** The APD (Figure 1) is a handheld unit with a rotating wheel that perturbs airflow and calculates  $R_r$  for each perturbation based on the measured changes in airflow rate and air pressure. It consists of a pneumotachometer with a cone on one end for attachment to an air filter and a disposable mouthpiece, and a rotating segmented wheel on the opposing end. Rotation of the segmented wheel in front of the flow path periodically diminishes airflow and raises oral pressure compared with the unperturbed signal. The wheel self-adjusts to be commensurate with changing resistances within the device and the respiratory system.<sup>14</sup> Pressure transducers on either side of the pneumotachograph's screen sense differential pressure, which is used to determine airflow rate. A change in airflow, which is a continuous event detected just downstream of the mouth opening, is recorded by the device during the subsequent perturbations. The APD transfers data to a computer installed with custom software that continually monitors and records  $R_r$  in  $\text{cmH}_2\text{O}/\text{L}/\text{s}$  for each perturbation during inspiration and expiration.

Before use, the instrument self-calibrates when it is turned on and recognized by the computer. Data are recorded to a Microsoft Excel spreadsheet in sequential 1-minute trials, with each trial consisting of the following information: sequence of perturbations during inspiration and expiration, respectively; time of each perturbation (displayed to the nearest millisecond); air pressure (in  $\text{cmH}_2\text{O}$ ) for each perturbation; airflow (in  $\text{L}/\text{s}$ ) for each perturbation; and  $R_r$  (pressure/flow, in  $\text{cmH}_2\text{O}/\text{L}/\text{s}$ ). Values of  $R_i$  and  $R_e$  displayed on the computer following each trial represent the mean  $R_r$  of all perturbations during inspiration ( $R_i$ ) and during expiration ( $R_e$ ), respectively. In this study,  $R_r$  for each perturbation, rather than for each respiratory phase, was used in the analysis to better reflect instantaneous changes in GA.

**Glottal Area analysis.** GA analysis was conducted with *Kay's Image Processing System (KIPS)* software that comes standard with the KayPENTAX High-Speed Video System (model 9710).

### Procedure

On the day of the study, the participant practiced simulating breathing that is a characteristic of PVFM and visually monitored her vocal folds during inspiration and expiration using laryngoscopy. The goal was to narrow the glottis during inspiration and widen it during expiration. Likewise, the participant practiced simulated PVFM breathing with the APD in advance of data collection to ensure proper imitation.

Before insertion of the laryngoscope, the experiment began with the participant performing three separate 1-minute trials of RTB with the APD and while wearing a noseclip. This task was repeated twice to examine test-retest reliability during normal breathing and to verify that the participant's breathing while feigning PVFM differed from her normal breathing. The  $R_r$  data were stored in a computer spreadsheet for later comparison with  $R_r$  measures from simulated PVFM breathing. In preparation for the laryngoscopy procedure, the nasal mucosa was anesthetized with a cotton swab saturated with a 4% Xylocaine solution. A speech-language pathologist (SLP) passed the laryngoscope transnasally and simultaneously viewed the larynx on a monitor. The SLP operating the laryngoscope generally maintained a consistent distance between the distal tip of the endoscope and the

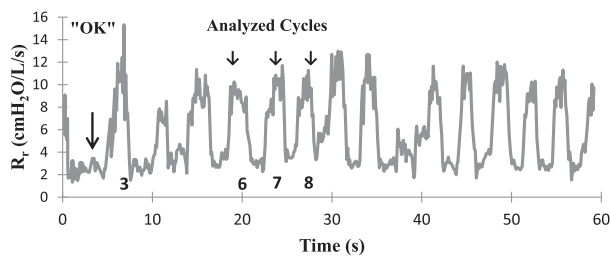


**FIGURE 2.** Breathing cycles generated from respiratory resistance ( $R_r$ ) values with three cycles selected for analysis of glottal area and  $R_r$ . The arrow pointing to the x-axis indicates the location of the trigger (OK) used for synchronizing the data signals.

vocal folds by keeping a consistent thumb-to-index finger grip on the scope while lightly resting the remaining fingers against the participant's nose. With the scope in position, the participant inserted the APD mouthpiece while maintaining a tight lip seal and wearing a noseclip to prevent transnasal air leakage throughout the experiment.<sup>20</sup> Should slight leakage around the nares housing the laryngoscope have occurred, a prior study by Lopresti et al<sup>20</sup> demonstrated that leakage between the lips and mouthpiece (represented by placing two 3.2-mm diameter tubes in the mouth) did not significantly change APD-measured  $R_r$ . A second SLP viewed both the monitor and computer screen while operating the computer and giving instructions. The participant then simulated laryngeal function characteristic of PVFM for a 1-minute trial. Following this, the laryngoscope, APD mouthpiece, and noseclip were removed. The laryngeal imaging digital file and the  $R_r$  data file were saved and electronically copied for future analysis.

### Data analysis

**Laryngeal imaging.**  $R_r$  and GA were compared directly by aligning the two waveforms for visual inspection. Video images were synchronized to the breathing cycles by first matching cycle 3. This cycle followed the examiner's verbal prompt "Okay" signaling the participant to begin PVFM-like breathing. This was followed by a robust inspiration (documented from the video recording) and a large increase in  $R_i$  (documented from the APD signal). The graph created from the  $R_r$  perturbation values is pictured in Figure 2, with cycles 3 and 6–8 identified.

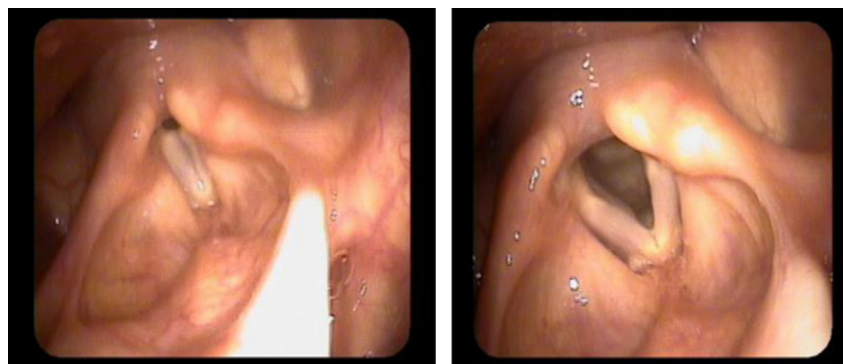


**FIGURE 3.** Maximal constriction of the laryngeal airway during inspiration (left) and minimal constriction during expiration (right) during feigned PVFM-like breathing.

Beginning with cycle 3, the frames corresponding to the start and end of each breathing phase were identified. The onset of each inspiratory phase was identified as the first frame with adductory motion of the vocal folds. The first frame with abductory motion signaled the beginning of expiration. This was considered highly accurate and acceptable for the purpose of this study. Figure 3 illustrates extreme vocal fold approximation during inspiration and vocal fold separation during expiration of feigned PVFM in this study.

Video frame numbers at the start of each inspiratory and expiratory phase were noted. After converting the video file into AVI (Audio/Video Interleaved) format at a sampling rate of 30 frames per second, breathing cycles 3–16 were chosen for frame-by-frame GA analysis. The first author performed the analysis after extensive practice and consensus with the second author. GA was segmented and measured in square pixels using *KIPS* software—accomplished by creating a montage of multiple frames, detecting GA, manually modifying the tracing of the glottis, and measuring the area between the vocal folds. The GA analysis used for this study included three complete breathing cycles (cycles 6–8) for a total of 341 frames. The remaining data could not be accurately analyzed for at least one of the following reasons: (1) fogging of the endoscopic image, (2) medial displacement of the arytenoid cartilages during inspiration that obscured the view of the glottis, and (3) indeterminate moments of inspiratory and expiratory onset and offset.

**Respiratory resistance.**  $R_i$  and  $R_e$  for each perturbation were identified for all 16 breathing cycles and graphed in a spreadsheet program. Each datum identified a particular moment of perturbation and its corresponding resistance value. By converting the perturbation time segments to frames (time multiplied by 30 to coincide with the sampling rate of the video frames) and rounding to the nearest whole number, breathing cycles 6–8 encompassed 337 frames—four fewer frames in the  $R_r$  analysis than in the GA analysis, resulting in a difference of 0.133 seconds. This discrepancy can be explained by the time lag caused by different sampling rates for  $R_r$  (~9 samples/s) and GA (30 frames/s).

### Statistical analysis

To explore the time-locked relationship between  $R_r$  and GA, cross-correlation analysis was conducted using *SPSS*, Version

18 (*Predictive Analytics Software Statistics*; SPSS, Inc., Chicago, IL) to determine a potential time delay between  $R_r$  and GA and to quantify the magnitude of the correlation. The cross-correlation coefficients (CCCs) were computed for 20 future and 20 previous values of  $R_r$  for each GA data point. This window of preceding and subsequent data points (ie, lags) was chosen to accommodate time delays between the two signals of more than one breathing cycle because each complete cycle comprises roughly 30 consecutive data points. The result of this analysis is a vector of nondifferenced cross-correlation function values computed between  $R_r$  and GA for each positive and negative lag position.

## RESULTS

### Respiratory resistance

Table 1 summarizes the results of  $R_i$  and  $R_e$  during RTB and feigned PVFM breathing in all 16 breathing cycles and in cycles 6–8 (the cycles selected for cross-correlation analysis between  $R_r$  and GA). During RTB,  $R_i$  values were comparable with those for  $R_e$ , with an inspiration-to-expiration ratio ( $R_i/R_e$ ) of 0.92. When feigning PVFM-like breathing,  $R_i$  and  $R_e$  were both greater than during RTB, with the greatest deviation occurring during inspiration, yielding an  $R_i/R_e$  ratio of 2.43.  $R_i$  was comparable across cycles 6–8, yet its average was 8% higher than the average  $R_i$  across all 16 cycles.  $R_e$  values in cycles 6 and 7 were comparable with each other and with the overall PVFM average, but were 54% lower on average than  $R_e$  for cycle 8. This  $R_e$  value for cycle 8 was  $\sim 2$  standard deviations (SDs) above the mean ( $\bar{x} = 3.31$ ,  $SD = 1.02$ ).

### Glottal area and respiratory resistance

GA and  $R_r$  were synchronized and plotted for breathing cycles 6–8 (Figure 4). The initial scatterplot of  $R_r$  over GA suggested a semilogarithmic correlation between the two variables (Figure 5); therefore,  $R_r$  is plotted versus  $\log_{10}(GA)$ . The logarithmic transformation of GA reduces the large spread in GA pixel values ranging from 81 to 11 448 square pixels during

three complete breathing cycles. When observing  $R_r$ , higher values (ie, peaks) are associated with inspiration and lower values (ie, valleys) with expiration. GA, in contrast, is larger during expiration and smaller during inspiration.  $R_r$  and  $\log_{10}(GA)$  exhibit similar periodicity in the three evaluated cycles lasting 11.25 seconds (Figure 4).

Associations between  $R_r$  and GA were evaluated using cross-correlation analysis to determine time lag between each variable. The graph of the computed CCCs versus lag number (Figure 6) illustrates the same periodicity that was observed in the  $R_r$  and  $\log_{10}(GA)$  graphed signals in Figure 4.

The computed CCCs for each of the 20 forward and backward lag positions show that the largest CCC occurs at a lag position of +2. A CCC of  $-0.824$  shows a strong negative linear relationship between changes in  $\log_{10}(GA)$  and changes in  $R_r$  (ie, an increase in GA leads to a reduction in  $R_r$ ). The lag position of +2 indicates that the cyclic changes in  $\log_{10}(GA)$  occur approximately two data points ahead of the measured  $R_r$  and confirm that both parameters are nearly synchronized. A time delay of  $\sim 0.2$  seconds for  $R_r$  is calculated by multiplying the sampling rate of the measurement (0.118 seconds) by the lag number (2).

## DISCUSSION

The results of this study support the hypothesized inverse relationship between GA and  $R_r$  during feigned PVFM breathing. Cross-correlation analysis revealed a strong negative correlation between GA and  $R_r$  with a lag of approximately 0.2 seconds. This analysis confirms that  $R_r$  decreases when GA increases and that changes in GA precede changes in  $R_r$ . Although it is logical that the change in GA occurs first, the lag time was somewhat greater than expected.

There are two possible explanations for the slight asynchrony between GA and  $R_r$ . First, the onsets of inspiration and expiration were marked by the first observed video frame signaling vocal fold adduction and abduction, respectively. Human error may have contributed to a misidentification of each breathing phase within a few video frames. Also, synchrony of GA and  $R_r$  may have been impacted by a time delay between the beginning of vocal fold movement and the measurement of air pressure and flow by the APD because a change in airflow detected at the mouth is not recorded by the device until the subsequent perturbation. This delay can be as great as 100 milliseconds, which is equivalent to the average period between adjacent perturbations. Overall, however, the lag between the data signals was small and was accounted for in the calculation of the CCC. Additionally, the small time delay is of no real consequence when using the APD for PVFM diagnosis and monitoring because it takes much longer than 0.2 seconds just to put the APD in place to make a measurement.

This is the first known attempt to correlate APD-measured  $R_r$  with GA and as such presented challenges. The authenticity of this study would be improved if it was performed with a participant symptomatic of PVFM at the time of the study. Most of the patients presenting to the first author's clinic required an exercise task to induce signs of PVFM; however, simultaneous

**TABLE 1.**  
Inspiratory and Expiratory Resistance During RTB and Feigned PVFM Breathing

Condition	Inspiratory Resistance (cmH <sub>2</sub> O/L/s)	Expiratory Resistance (cmH <sub>2</sub> O/L/s)
<b>RTB</b>		
Trial 1	1.77	1.84
Trial 2	1.61	1.81
Trial 3	1.61	1.72
Mean	1.66	1.79
<b>PVFM breathing</b>		
Cycles 1–16	8.01	3.31
Cycle 6	8.58	3.11
Cycle 7	8.80	3.85
Cycle 8	8.67	5.26

Abbreviations: RTB, resting tidal breathing; PVFM, paradoxical vocal fold motion.



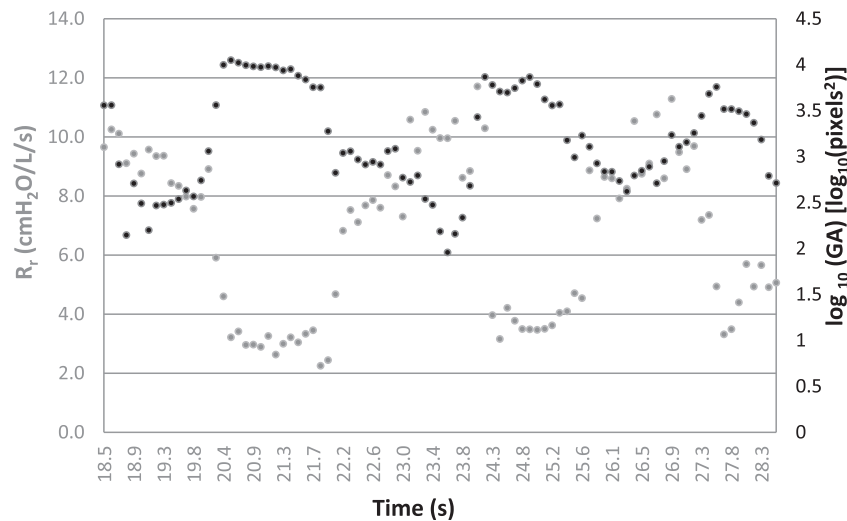


**FIGURE 4.** Respiratory resistance ( $R_r$ , gray) and log-transformed glottal area [ $\log_{10}(\text{GA})$ , black] waveforms for PVFM-like breathing cycles 6–8.

placement of the nasal endoscope and the APD does not easily accommodate performing exercise. Likewise, the intermittent nature of PVFM cannot guarantee the desired response. Thus, even though the participant in this study did not suffer from PVFM disorder, the essential characteristic of PVFM was reproduced. The participant purposely exaggerated glottal constriction during inspiration so that the two phases of the respiratory cycle were distinctly different. This amount of glottal constriction sometimes interfered with clear visualization of the laryngeal airway that was required for GA analysis and limited the number of cycles available for the analysis. The authors acknowledge that patients presenting with PVFM may experience more subtle glottal changes than those produced by the participant in this study.

There were additional challenges encountered in this study: (1) synchronizing the laryngeal recording with the start of the APD trial, which in future studies will be remedied by using an external beep tone; (2) identifying the beginning and ending

of each breathing phase from the laryngeal images, which can be solved by using respiratory inductance plethysmography simultaneously with laryngoscopy and the APD to clearly define breathing phases; (3) controlling for the distance between the scope tip and the vocal folds, which can be facilitated by marking the place on the scope where it entered the nose and aligning the mark with the nasal opening. Finally, analyzing more breathing cycles than what was done for this study using healthy participants feigning PVFM and participants who have the disorder will inevitably provide a better understanding of the relationship between  $R_r$  and GA.

Although the procedure of laryngoscopy during exercise is ideal for diagnosing PVFM, its clinical utility has drawbacks. It is uncomfortable for patients, carries increased medical risks, and therefore demands high-level medical support. Moreover,

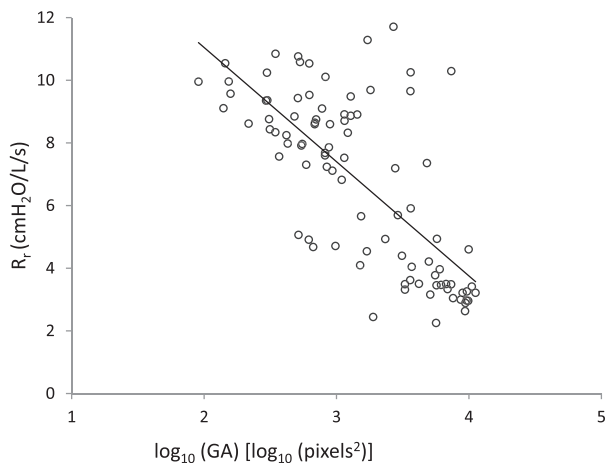


**FIGURE 5.** Respiratory resistance ( $R_r$ ) and log-transformed glottal area [ $\log_{10}(\text{GA})$ ] for the three complete breathing cycles (6–8) shown in Figure 4. The linear trend line shows that  $R_r$  gradually decreases as GA increases.

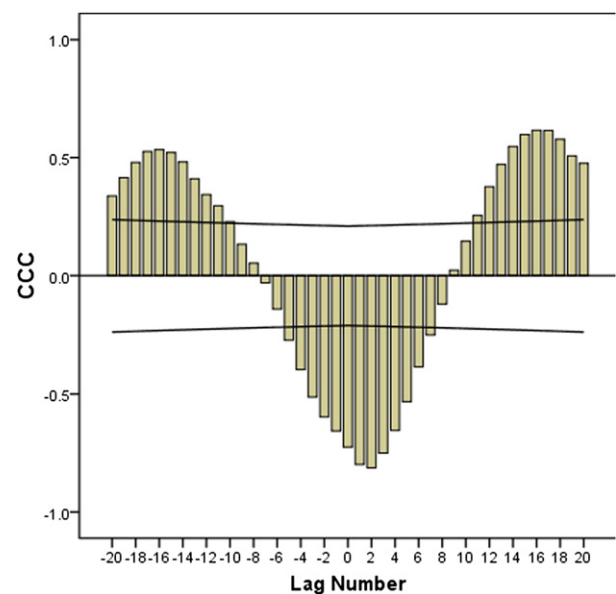


**FIGURE 6.** Cross-correlation coefficients for respiratory resistance and log-transformed glottal area plotted against lag position. Lines indicate confidence limits of two standard errors at each lag position.

measuring GA frame-by-frame is very time consuming, even for research purposes. Thus, one of the challenges facing present research and clinical management of PVFM is finding a less invasive and more efficient way to discern changes in GA. Inspiratory and expiratory resistance measured with a portable, hand-held APD seems to be a good alternative to detect changes in the laryngeal airway during PVFM episodes. This study provided evidence validating the use of the APD for detecting changes in GA. Although other sources of respiratory resistance could have contributed to the result, the marked and deliberate change in GA is most certainly the primary contributor to the observed changes in  $R_r$ . Subsequent studies are needed to investigate test-retest reliability of  $R_r$  measurements in athletes who have been diagnosed with PVFM and in healthy control athletes.

### Acknowledgments and Disclaimer

This research represents a portion of a doctoral dissertation by Dr. Gallena directed by Drs. Tian and Solomon and could not have been completed without support from the Department of Hearing and Speech Science, University of Maryland. The views expressed in this article are those of the authors and do not reflect the official policy of the Department of Army, Department of Defense, or U.S. Government.

### REFERENCES

1. Beaty MM, Wilson JS, Smith RJ. Laryngeal motion during exercise. *Laryngoscope*. 1999;109:136–139.
2. Bent JP, Miller DA, Kim JW, Bauman NM, Wilson JS, Smith RJ. Pediatric exercise-induced laryngomalacia. *Ann Otol Rhinol Laryngol*. 1996;105:169–175.
3. Christopher KL, Morris MJ. Vocal cord dysfunction, paradoxical vocal fold motion, or laryngomalacia? Our understanding requires an interdisciplinary approach. *Otolaryngol Clin North Am*. 2010;43:43–66.
4. Dion GR, Eller RL, Thomas RF. Diagnosing aerodynamic supraglottic collapse with rest and exercise flexible laryngoscopy. *J Voice*. 2012;26:779–784.
5. Richter GT, Rutter MJ, deAlarcon A, Orvidas LJ, Thompson DM. Late-onset laryngomalacia: a variant of disease. *Arch Otolaryngol Head Neck Surg*. 2008;134:75–80.
6. Mathers-Schmidt BA. Paradoxical vocal fold motion: a tutorial on a complex disorder and the speech-language pathologist's role. *Am J Speech Lang Pathol*. 2001;10:111–125.
7. McFadden ER, Zawadski DK. Vocal cord dysfunction masquerading as exercise-induced asthma. *Am J Respir Crit Care Med*. 1996;153:942–947.
8. Brugman SM, Simons SM. Vocal cord dysfunction: don't mistake it for asthma. *Phys Sportsmed*. 1998;26:63–74.
9. Heinle R, Linton A, Chidekel AS. Exercise-induced vocal cord dysfunction presenting as asthma in pediatric patients: toxicity of inappropriate inhaled corticosteroids and the role of exercise laryngoscopy. *Pediatr Asthma Allergy Immunol*. 2003;16:215–224.
10. Tervonen H, Niskanen MM, Sovijärvi AR, Hakulinen AS, Vilkman EA, Aaltonen L. Fiberoptic videolaryngoscopy during bicycle ergometry: a diagnostic tool for exercise-induced vocal cord dysfunction. *Laryngoscope*. 2009;119:1776–1780.
11. Gartner-Schmidt JL, Rosen CA, Radhakrishnan N, Ferguson BJ. Odor provocation test for laryngeal hypersensitivity. *J Voice*. 2008;22:333–338.
12. Rundell KW, Slee JB. Exercise and other indirect challenges to demonstrate asthma or exercise-induced bronchoconstriction in athletes. *J Allergy Clin Immunol*. 2008;122:238–246.
13. Rundell KW, Spiering BA. Inspiratory stridor in elite athletes. *Chest*. 2003;123:468–474.
14. Silverman NK, Johnson AT. Design for a stand-alone airflow perturbation device. *Int J Med Implant Device*. 2005;1:139–150.
15. Silverman NK, Johnson AT, Scott WH, Koh FC. Exercise-induced respiratory resistance changes as measured with the airflow perturbation device. *Physiol Meas*. 2005;26:29–38.
16. Balkissoon R. Vocal cord dysfunction, gastroesophageal reflux disease, and nonallergic rhinitis. *Clin Allergy Immunol*. 2007;19:411–426.
17. Johnson A, Scott W, Russek-Cohen E, Koh FC, Silverman NK, Coyne KM. Resistance values obtained with the airflow perturbation device. *Int J Med Implant Device*. 2007;2:45–58.
18. Johnson AT, Berlin HM, Prunell SA. Perturbation device for non-invasive measurement of airway resistance. (Abstract). *Med Instrum*. 1974;8:141.
19. Lausted C, Johnson A. Respiratory resistance measured by an airflow perturbation device. *Physiol Meas*. 1999;20:21–35.
20. Lopresti ER, Johnson AT, Koh FC, Scott WH, Jamshidi S, Silverman NK. Testing limits to airflow perturbation device (APD) measurements. *Biomed Eng Online*. 2008;7:28–50. doi:10.1186/1475-925X-7-28.